Estimating Ultraviolet Radiation From Global Horizontal Irradiance

Aron Habte, Manajit Sengupta, Christian A. Gueymard, Ranganath Narasappa, Olivier Rosseler, and David M. Burns

***Abstract*—Terrestrial ultraviolet radiation (UV) radiation is a primary factor contributing to the degradation of photovoltaic (PV) modules' efficiency and reliability over time. Therefore, accurate knowledge of terrestrial UV incident on the surface of the PV materials is essential to understand the degradation of PV modules and provide reliable assessment of their service life. As PV is deployed in various climate zones, it is crucial that terrestrial UV information is available at various locations. However, the availability of terrestrial UV data—measured or modeled—is extremely limited. On the other hand, total solar irradiance (TS) datasets are relatively abundant. In this study, the National Renewable Energy Laboratory, its industry partners, and ASTM's International Subcommittee on Radiometry and Service Life Prediction are developing a simple method to estimate the clear-sky terrestrial UV irradiance (280–400 nm, 295–400 nm, 285–385 nm, or 295–385 nm) from total irradiance data (280–4000 nm). The goal is to provide reliable estimates of the UV received by samples as a function of location, orientation, tilt, and airmass, thus encompassing a variety of conditions. The Simple Model of the Atmospheric Radiative Transfer of Sunshine (SMARTS) model is used to estimate the UV:TS ratio under various scenarios, and examines the influences of atmospheric constituents, such as aerosols, precipitable water vapor or ozone, and of the local surface characteristics (albedo), on the predicted UV.**

***Index Terms*—Global radiation, PV degradation, standards, UV.**

I. Introduction

As SOLAR energy conversion systems become prevalent, accurate knowledge of the incoming solar irradiance is now necessary to evaluate the reliability and degradation of these systems. This is in addition to the more conventional use of solar resource data for design and performance evaluation. The service life and durability of solar systems depend on their resistance to physical and chemical changes. These changes occur because of exposure to solar radiation in combination with heat and various states of water [1], [2]. Solar radiation—specifically ultraviolet (UV) radiation, as one of the major stress factors—plays a significant role in the dissociation of polymer bonds in coatings, and discoloring of pigments [2], [3]. Therefore, obtaining accurate solar radiation data is important to accurately predict the service life and durability of the materials that make up the solar conversion systems such as photovoltaic (PV) modules.

Solar radiation covers a wide spectral range. A small portion of this spectrum is UV radiation, which consists of those wavelengths between 280 and 400 nm [3]. UV plays an important role in altering the properties and accelerating the degradation of materials. This is particularly the case for the transparent cover (including coatings) and encapsulant of PV modules [4]. The ability to quantify, through measurement or modeling, the UV component of the solar spectrum is essential to adequately characterize the long-term degradation effects on these materials.

Various national and international groups, such as ASTM International or the International Electrotechnical Commission, are working toward quantifying the incident UV radiation for indoor and/or outdoor exposure applications. However, measured UV data are not readily available because of the paucity of monitoring stations. It is therefore necessary to determine the UV irradiance through modeling. Since location-specific total (broadband) solar (TS) irradiance data sources are abundant, estimating UV from TS appears to be a good alternative.

Most studies so far were concerned with the evaluation of the *erythemal* UV for biological or health applications. In contrast, this study investigates the *total* UV irradiance on horizontal and tilted surfaces by developing a model of the UV:TS ratio using simulations obtained with the Simple Model of the Atmospheric Radiative Transfer of Sunshine (SMARTS) spectral model [5], [6] for various locations around the world.

II. Method

Multiple SMARTS simulations are performed to estimate a multitude of UV:TS ratios as a function of location, tilt, orientation, airmass (AM), surface albedo, and atmospheric constituents such as aerosols, water vapor, or ozone. These modeled UV:TS ratios can then be multiplied by available TS data to obtain the desired UV irradiance. If TS is not measured locally, modeled estimates (which are typically of reasonable accuracy) can be used instead. Representative locations are selected here

Manuscript received May 20, 2018; revised September 9, 2018; accepted September 17, 2018. This work was supported by the U.S. Department of Energy Office of Energy Efficiency and Renewable Energy Solar Energy Technologies Office under Contract DE-AC36-08GO28308. *(Corresponding author: Aron Habte.)*

A. Habte, M. Sengupta, and R. Narasappa are with the National Renewable Energy Laboratory, Golden, CO 80401 USA (e-mail: aron.habte@nrel.gov; manajit.sengupta@nrel.gov; Ranganath.Narasappa@nrel.gov).

C. A. Gueymard is with Solar Consulting Services, Colebrook, NH 03576 USA (e-mail: Chris@SolarConsultingServices.com).

O. Rosseler is with Saint-Gobain Research North-America, Northborough, MA 01532 USA (e-mail: Olivier.Rosseler@saint-gobain.com).

D. M. Burns is with 3M Weathering Research Center, St. Paul, MN 55144-1000 USA (e-mail: dmburns@mmm.com).

Color versions of one or more of the figures in this paper are available online at http://ieeexplore.ieee.org.

Digital Object Identifier 10.1109/JPHOTOV.2018.2871780

TABLE I
LOCATION INFORMATION AND ASSOCIATED NUMERICAL COEFFICIENTS OBTAINED BY LEAST-SQUARES FITTING (280–400 nm) UNDER HORIZONTAL (ZERO TILT) CONDITIONS

Station	Lat. (°)	Long. (°)	Elev. (m)	m_4	m_3	m_2	m_1	m_0
Birdsville, Australia	-25.9	139.3	46	1.79E-06	-8.39E-05	1.47E-03	-1.01E-02	7.09E-02
CEI Qiong Hai, HaiNan province, China	19.2	110.5	62	2.84E-06	-1.27E-04	1.95E-03	-1.11E-02	7.05E-02
CEI Turpan, XinJiang province, China	42.9	89.8	10	3.25E-06	-1.45E-04	2.22E-03	-1.22E-02	6.86E-02
Case Western Reserve University (CWRU), OH, USA	41.5	-81.6	200	2.53E-06	-1.15E-04	1.87E-03	-1.18E-02	7.05E-02
Fairbanks, AK, USA	64.8	-147.7	136	1.04E-06	-6.01E-05	1.26E-03	-9.98E-03	7.76E-02
KACST Riyadh, Saudi Arabia	24.9	46.4	740	3.30E-06	-1.46E-04	2.17E-03	-1.16E-02	7.02E-02
Miami, FL, USA	25.6	-80.5	30	2.30E-06	-1.09E-04	1.82E-03	-1.15E-02	7.26E-02
Nauru	-0.5	166.9	7	1.46E-06	-7.52E-05	1.38E-03	-9.76E-03	7.38E-02
NREL-Golden, CO, USA	39.7	-105.2	1829	1.97E-05	-5.39E-04	5.26E-03	-2.18E-02	7.96E-02
Petrolina, Brazil	-9.4	-40.5	370	1.73E-06	-8.53E-05	1.52E-03	-1.04E-02	7.26E-02
Phoenix, AZ, USA	33.9	-112.2	395	1.97E-06	-9.41E-05	1.62E-03	-1.08E-02	7.09E-02
Pretoria, South Africa	-25.8	28.3	1449	2.91E-06	-1.28E-04	2.04E-03	-1.27E-02	7.07E-02
Sanary, France	43.1	5.8	110	2.50E-06	-1.14E-04	1.86E-03	-1.18E-02	6.97E-02
Singapore	1.3	103.8	30	3.10E-06	-1.37E-04	2.09E-03	-1.19E-02	7.12E-02
Toravere, Estonia	58.3	26.5	70	2.16E-06	-9.92E-05	1.67E-03	-1.10E-02	6.84E-02

Fig. 1. Representative locations included in this study.

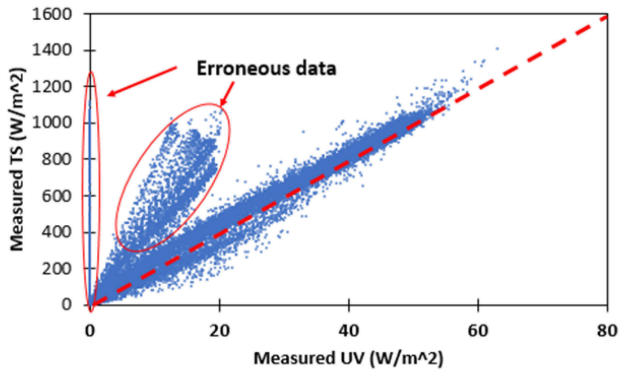

Fig. 2. Example of erroneous data from the Phoenix, AZ, 2015 dataset removed during the quality assessment process.

(see Fig. 1). They are from both the Northern and Southern Hemispheres, and include various latitudes and elevations, as well as differing atmospheric conditions and multiple climatic zones [4]. Additionally, some of these locations are often used by solar energy or weathering and durability organizations to predict the service life of various materials. The SMARTS outputs for these or other locations can be directly compared with what would be obtained under the conditions pertaining to the ASTM G173 standard spectrum [7], since the latter was also developed with SMARTS.

At the earth surface, the irradiance is strongly affected by the AM factor, a pure function of the sun's zenith angle, which characterizes the sun geometry [8]. Using the SMARTS model, numerous AM-dependent irradiance simulations are first generated for the locations under study.

The results obtained from the model are validated below using ground-measured total UV. Data from seven high-quality locations representing various climatic conditions are used for this validation process. These stations use various radiometer types to sense UV (see Table I). For example, the National Oceanic and Atmospheric Administration (NOAA) UV network sites are equipped with a scanning SUV-100 spectroradiometer manufactured by Biospherical Instruments, Inc. [9]. For these locations, the spectral irradiance over 290–400 nm is integrated to obtain the broadband UV, which is then used to validate the modeled UV obtained from this study.

A. Data Quality Assessment of Measured Ultraviolet for Use in the Validation Process

A preliminary data quality assessment is performed at each site, using a simple regression and standard deviation analysis to remove outliers and/or erroneous data between the measured *TS* and *UV* (see Table I). A scatterplot of these two measurements normally shows a linear relationship. Using these relationships, erroneous data can be detected and removed. No additional quality assessment is necessary at those stations that provide quality-controlled data, such as those of the Biospherical or NOAA networks. The SUV-100 observations need to be corrected for cosine error, however [9], [10]. At the NREL station, the UV measurements are not corrected because they are calibrated on a regular basis using spectroradiometers traceable to the National Institute of Standards and Technology. All NREL instrumentation is maintained daily (except weekends and holidays), and the site personnel transfers the daily maintenance records into a database. For these reasons, the NREL station had few outliers and/or erroneous data compared with the Phoenix or Miami stations (see Table I). In the case of the Phoenix station, Fig. 2 shows an example of erroneous data removed at this stage. The errors could be because of malfunction or to moving the UV sensor to another platform with a different tilt angle during a certain period.

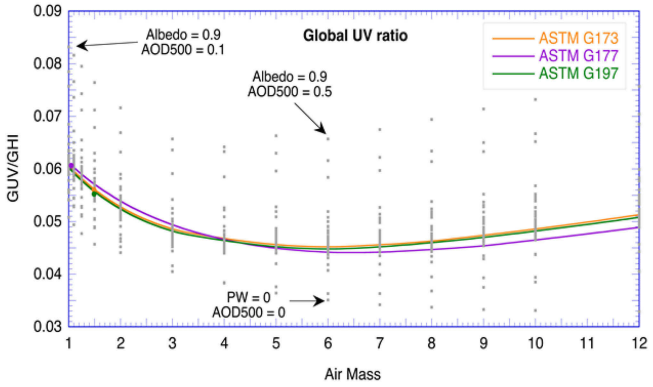

Fig. 3. R_{uv} as a function of AM for the fixed atmospheric conditions of three existing ASTM standards (colored lines), and for other conditions (gray dots). A horizontal receiver is assumed.

III. Results and Discussion

The UV:TS ratio method can be employed for locations where measured or modeled TS data are available. By multiplying the ratio obtained from the SMARTS model output by available TS data, the corresponding UV irradiance can be estimated at that location and under specified conditions. The method thus consists in estimating the modeled UV irradiance, UV_m, using

$$UV_m = TS_m * R_{uv} \tag{1}$$

where

$$R_{uv} = \frac{UV_s}{TS_s} \tag{2}$$

and where TS_m (W/m^2) is the measured or modeled TS irradiance under similar conditions under which R_{uv} was derived. Hence, TS_m can be either the global horizontal irradiance (GHI) or global tilted irradiance (GTI), depending on the geometry of the receiver. UV_S and TS_S are the total UV irradiance and total shortwave irradiance estimated with SMARTS, respectively (W/m^2). In what follows, UV_S is referred to as global UV (GUV) in the case of a horizontal receiver. Finally, R_{uv} is the UV:TS ratio obtained from SMARTS, e.g., GUV/GHI for a horizontal receiver. If R_{uv}, a function of AM, is multiplied by the measured or modeled GHI, the modeled UV on a horizontal surface is obtained. For instance, both measured and modeled GHI data can be obtained from NREL's websites (https://midcdmz.nrel.gov and https://nsrdb.nrel.gov, respectively).

In Fig. 3, results are obtained using the conditions pertaining to ASTM G173, G177, and G197 (orange, purple, and green lines, respectively). The relative AM is varied between 1 (overhead sun) and 12 (86° zenith angle or 4° sun elevation). Throughout the range of AM investigated here (1–12), the UV:TS ratio varies only slightly, from ≈0.045 to 0.060, when the atmospheric conditions are fixed to those stipulated in the standards. Additional points show the sensitivity of R_{uv} on changing atmospheric or environmental conditions. Low ratios correspond to low aerosol optical depth (AOD) and/or low precipitable water (PW), whereas high ratios are related to high surface albedo and/or high AOD. There are additional second-order effects from ozone, pressure (site elevation), and aerosol type.

A. Model Formulation

The UV:TS ratio is modeled using *mean-annual* atmospheric conditions for the 15 locations of Table I. The ratios are calculated from AM using (2), and a least-squares fitting technique is applied to match all curves in Fig. 4.

For instance, using the prevailing *mean-annual* atmospheric conditions at NREL's Solar Radiation Research Laboratory (SRRL) measurement station in Golden, Colorado (see Fig. 4), the variation of the ratio as a function of AM appears to be similar to that in Fig. 3. A good fit, valid for any AM, *m*, below 65 (zenith angles less than ≈92°) is obtained from a fourth-order polynomial for each of the 15 locations

$$UV_m = TS_m \left(\sum_{0}^{4} m_i AM^i \right) \tag{3}$$

where *AM* is the air mass and m_i are numerical coefficients (see Table I and Fig. 4).

B. Validation Using Horizontal Sensors

In Fig. 6, the modeled UV_m results for one specific clear winter day are compared with 1-min UV measurements using two different UV radiometers (Eppley Lab TUVR and Kipp & Zonen CUV4) at the SRRL location. The two radiometers sense the UV from ≈300 to 385 nm, but at SRRL they are calibrated against a spectroradiometer to represent the 280–400 nm spectral range. This comparison shows relatively good agreement, with some apparent model overestimation. Around solar noon, the measured and modeled UV differ by ≈2.2 W/m^2, or ≈8%. The difference might be attributed to the use of mean-annual input values (rather than those pertaining to that specific day) in the model, model inadequacies, and experimental uncertainty (e.g., caused by the special calibration procedure described above).

Two separate UV radiometers are used here to check for measurement consistency. It is observed that the instrument-induced difference is well within the combined experimental uncertainty (see Fig. 5).

For a longer term validation, Fig. 6 shows a scatter-plot comparison between the measured (CUV4 instrument) and modeled UV for all-sky conditions during a 50-day period (December 1, 2017 to January 19, 2018) at NREL-SRRL. The area was covered with snow during a few days. Because a higher surface albedo can significantly increase the backscattering contribution in the UV compared with the whole solar spectrum, conditions for which the measured albedo was larger than 0.5 are identified separately, and indeed demonstrate a different behavior.

Similarly, Fig. 7 compares the modeled results with their measured counterpart under "clear-sky" conditions, defined here by a total cloud cover (observed with a sky imager) of less than 10%. The correlation between the modeled and measured UV irradiance is highly significant ($r^2 = 0.995$), which provides confidence in the simple clear-sky model developed here.

Moreover, in Fig. 8, the modeled UV_m results for one year (August 2016 to August 2017) are compared with average values of hourly UV measurements from the two different UV radiometers at the SRRL location. The modeled estimates show good

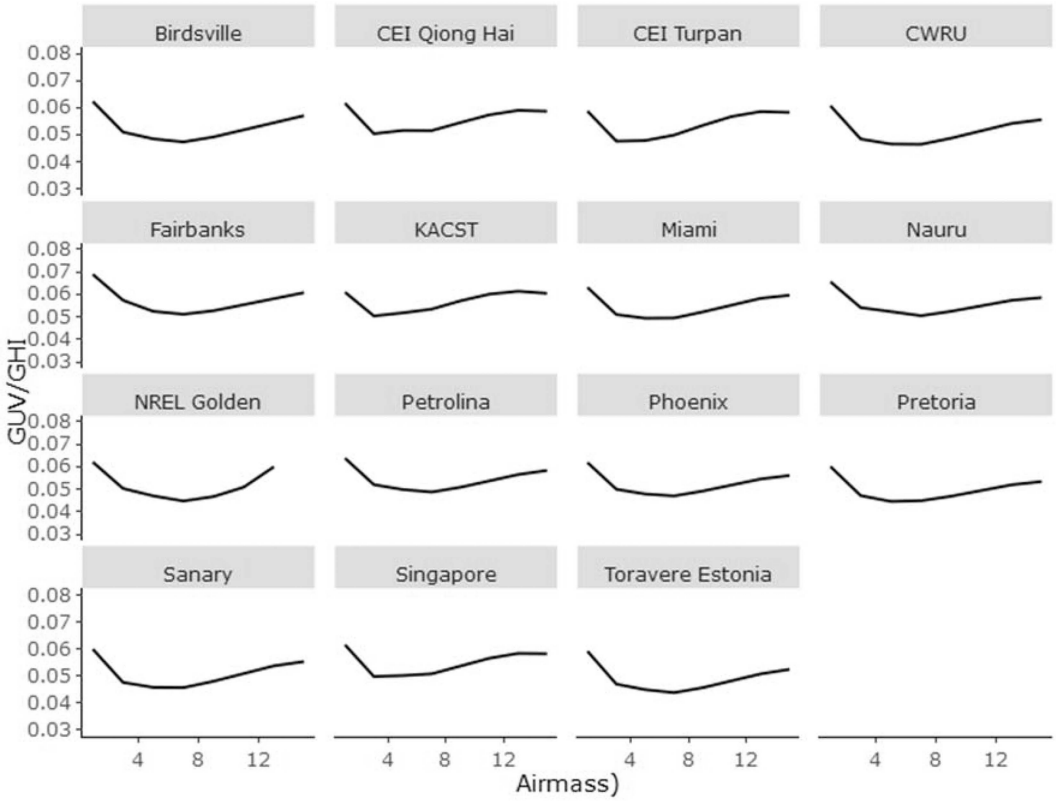

Fig. 4. R_{uv} as a function of AM for mean annual fixed atmospheric conditions (prevailing conditions) at 15 world locations (280–400 nm).

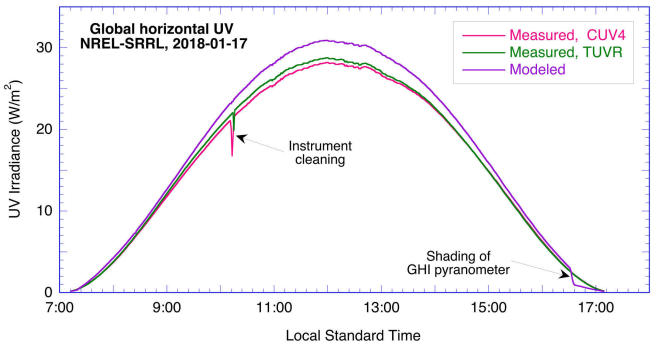

Fig. 5. Comparison of measured and modeled UV horizontal irradiance under clear-sky conditions at SRRL (Golden, CO).

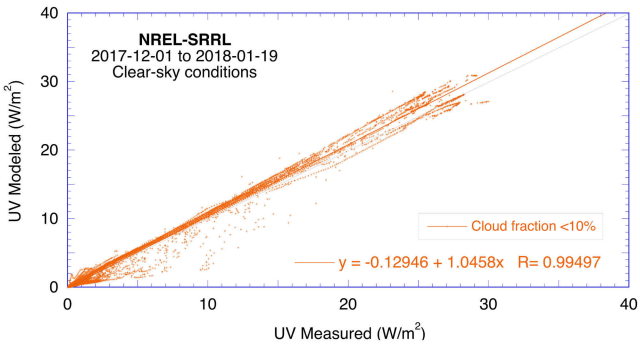

Fig. 7. Modeled versus measured 1-min UV global irradiance under clear-sky winter conditions at SRRL.

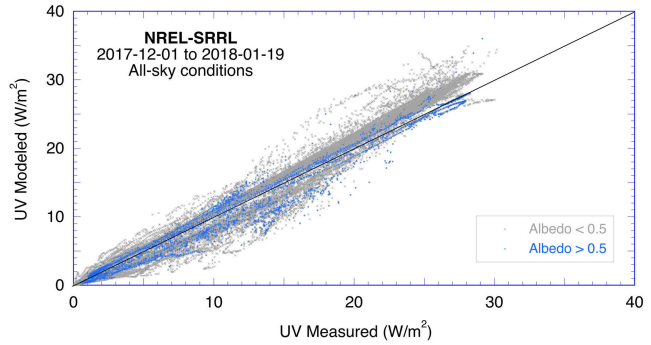

Fig. 6. Modeled versus measured 1-min UV irradiance under all-sky conditions at SRRL for low and high surface albedo conditions.

agreement with the measured UV data, with a slight overestimation of the higher irradiance values. These results are very important because they show that R_{uv} is actually not significantly affected by cloudiness, at least for the conditions of the SRRL station. Hence, the results obtained under clear-sky conditions with SMARTS are generally valid, pending additional validation at sites in different climates.

Most of the hourly differences are within ± 2 W/m^2, as shown in Fig. 9. There are only a few outliers outside of the ± 4 W/m^2 range, which could be related to unusual combinations of atmospheric conditions or radiometer maintenance issues.

To further evaluate the model's performance, irradiance observations from various other locations have been used.

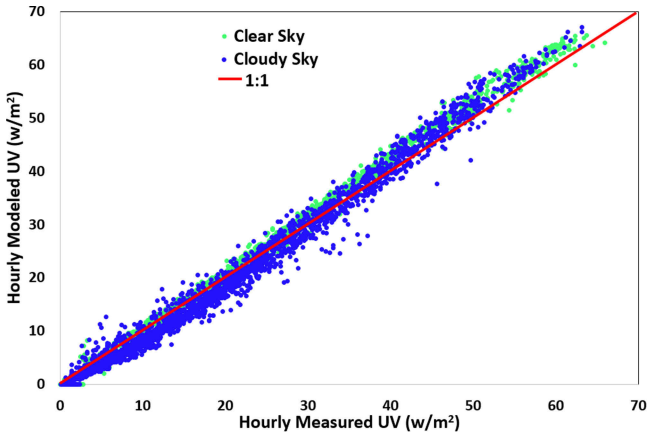

Fig. 8. Hourly modeled versus measured GUV irradiance under clear- and cloudy-sky conditions at SRRL, using one year of data.

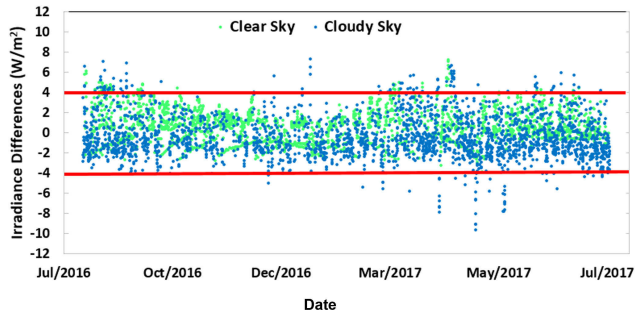

Fig. 9. Hourly modeled versus measured GUV irradiance differences under clear-sky and cloudy-sky conditions at SRRL.

Scatterplots are shown in Fig. 10, revealing that the modeled UV estimated here is reasonably close to the measured values. The difference between the modeled and measured values is small: for the four locations, the average root-mean-square error (RMSE) and mean bias error (MBE) are 3.1 and ≈–0.6 W/m^2, respectively. The coefficient of determination, r^2, is above ≈95% for all locations, which provides confidence on how well the model is replicating the measured data. There is a slight overestimation of the modeled values, which could be explained by the use of mean-annual atmospheric conditions as inputs to SMARTS. Some of the input variables, such as PW or AOD, may be estimated too low for those higher UV irradiance values. Moreover, radiometers such as the Eppley PSP have higher cosine error at high solar zenith angles [11]. This could have more effect at stations such as Alaska or Palmer, where the vast majority of solar zenith angles remain above 60° during the year.

The scatter appears larger at Kailua Kona, which can be explained by the use of a UV sensor with limited accuracy, considering the manufacturer's specification of a calibration uncertainty as high as 10%.

Additional SMARTS simulations are performed to provide UV over spectral ranges such as 285–385 nm or 295–385 nm, because these ranges are typically reported and used in many weathering and durability applications. A different set of coefficients generated by least-squares fitting applies to these UV ranges. Restricting the UV to the 285–385 nm waveband significantly reduces the irradiance compared with the 280–400 nm definition (reported in ASTM G177 [12]), which can be a source of confusion or error.

C. Model Formulation for Tilted Sensors

The model and validation discussed thus far apply to horizontal surfaces and UV light in the 280–400 nm spectral range. Most of the applications intended here rather deal with tilted surfaces. Furthermore, radiant UV doses in weathering and durability studies are reported in the 295–400 nm or 295–385 nm range. This section investigates the impact of tilt angle and UV spectral range on the $R_{\rm uv}$ ratio.

The $R_{\rm uv}$ ratio is generated for various tilt angles using SMARTS, and then applied to measured or modeled GTI for multiple locations. These results are validated here using data from the Phoenix and Miami stations, as discussed next.

Coefficients of GTI $R_{\rm uv}$ for various wavelength ranges are then derived

$$R_{uv} = \frac{\mathrm{GTI}\, UV_s}{\mathrm{GTI}_s}. \tag{4}$$

Similarly, to (3), a fourth-order polynomial fit is developed for the 280–400, 295–400, and 295–385 nm wavelength ranges. These fits are valid for any AM, *m*, below 65 (zenith angles less than ≈92°), as shown in (5).

As mentioned previously, the availability of UV data is extremely limited or even non-existent where solar technologies are deployed. Similarly, GTI data cannot be found easily for all possible geometries of interest in UV degradation applications. On the other hand, GHI can easily be found in the typical meteorological year (TMY) data disseminated publicly by NREL, for instance. Using a typical transposition model, the TMY GHI is first converted into GTI, from which the tilted UV irradiance can finally be obtained through

$$UV_m = \mathrm{GTI}_m \left(\sum_0^4 m_i AM^i \right). \tag{5}$$

With the assumption that cloudiness does not affect $R_{\rm uv}$, the method described here can be used with conventional TMY data to obtain a representative estimate of annual UV irradiation at hourly intervals. As an example, this is done in Table III for four U.S. locations in varied climates. For each site, the TMY GHI (TS_m) dataset is first converted to GTI for the desired tilt/azimuth, and then is used in conjunction with (5) to obtain the modeled UV over various spectral ranges, such as the 285–385 nm waveband.

In Table III, modeled UV irradiations (also referred to as "radiant doses") are compared with measured data. The model results are within 2–8% of the measured values. To put this result into perspective, the yearly variation of natural sunlight intensity is 1–14%, based on the measured UV dose at tilts of 5°, 45°, and latitude tilt in both Miami and Phoenix during 2015–2017 (based on data kindly provided by Atlas-MTT).

Table III also includes results provided in other studies based on actual measurements on near-horizontal or tilted surfaces for comparison. Notice that the wider the wavelength range, the

TABLE II
INFORMATION ABOUT VALIDATION STATIONS

Station	Lat. (°)	Long. (°)	Elev. (m)	Type of Radiometer	Data Years	Eliminated data (%)	Time step (min.)	Tilt (°)	Source
Palmer Station, Antarctica	-64.767	-64.05	21	(UV) SUV-100 (290–400 nm); (TS) Eppley PSP	2009 2010	— —	15	0	http://www.esrl.noaa.gov/gmd/grad/antuv/
San Diego, CA	32.77	-117.2	22	(UV) SUV-100 (290–400 nm); (TS) Eppley PSP	2006 2007	— —	15	0	
Barrow, AK	71.32	-156.68	8	(UV) SUV-100 (290–400 nm); (TS) Eppley PSP	2013 2014 2015	— — —	15	0	http://uv.biospherical.com/
Kailua Kona, HI	19.73	-156.06	4	(UV) Apogee SU-100 (250–400 nm); (TS) Kipp & Zonen CMP11	2017 2018	3.0 1.9	60	0	https://midcdmz.nrel.gov/apps/go2url.pl?site=NELHA
NREL Golden, CO	39.741	-105.177	1829	(UV) Eppley TUVR, Kipp & Zonen CUV4 (280–400 nm); (TS) Kipp & Zonen CMP22	2016 2017	0.6 0	60	0	https://midcdmz.nrel.gov
Miami, FL	25.46	-80.501	30	(UV) Eppley TUVR (285–385 nm); (TS) Eppley PSP	2013 2014 2015	6.8 6.9 6.3	15	5, 26	Atlas Material Testing Technology
Phoenix, AZ	33.428	-112.583	395	(UV) Eppley TUVR (285–385 nm); (TS) Eppley PSP	2013 2014	2.5 3.5	15	5, 34	Atlas Material Testing Technology

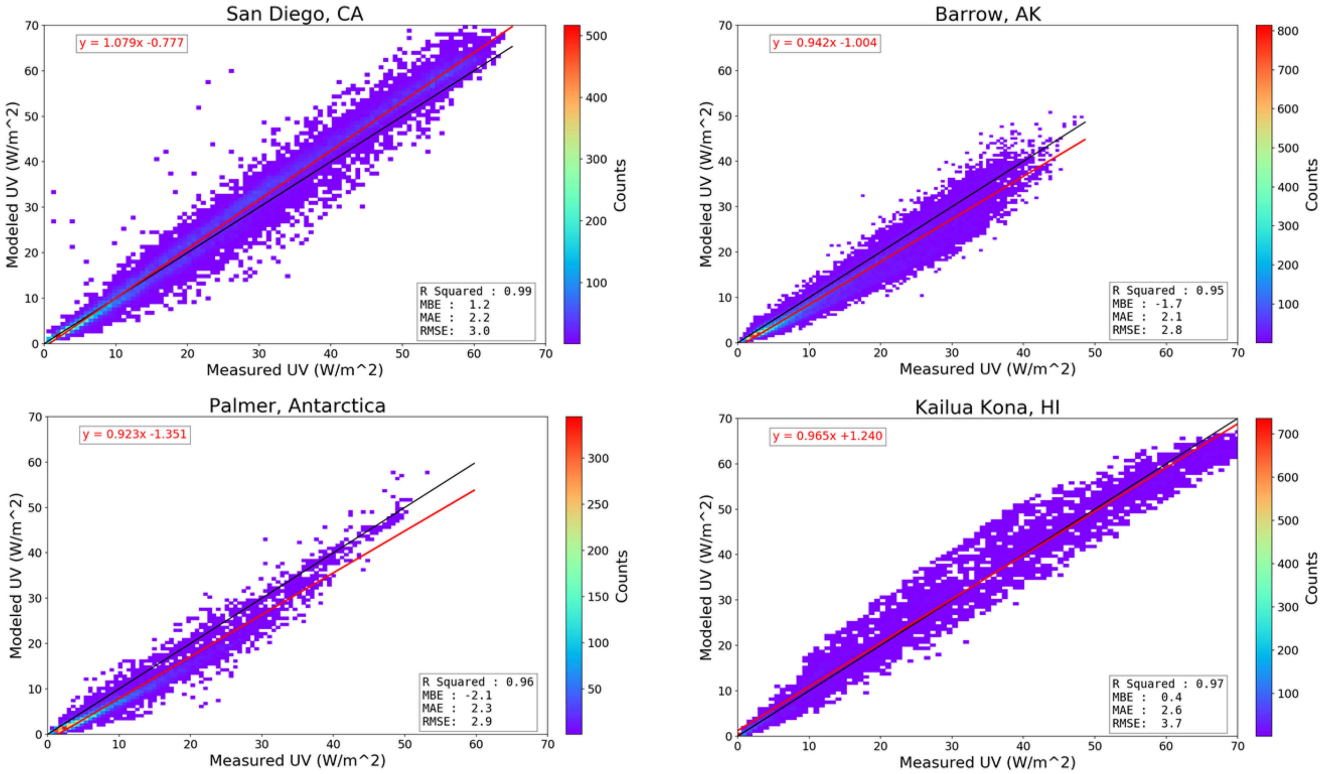

Fig. 10. Modeled versus measured GUV irradiance under all-sky conditions and zero tilt. RMSE and MBE values are in W/m^2. The black line is the 1:1 line and the red line is the regression line. The dot colors refer to a "density scale" from blue to red, with red showing the highest density of points. See Table II for years covered and time resolution for each location.

higher the radiant UV dose—calculated or measured. The spectral power distribution of natural sunlight at the surface of the earth contains negligible energy below 295 nm, hence the small difference between the 280–400 and 295–400 nm ranges. However, the 385–400 nm waveband contains significant energy, which explains the difference between the results for 295–400 and 295–385 nm. This underlines the importance of carefully defining the wavelength range used in calculated or measured UV data.

D. *Validation for Tilted Sensors*

In order to evaluate the tilted UV model's performance, and to examine the influence of the SMARTS input variables, measured tilted UV irradiances from two locations are compared with the corresponding modeled tilted UV. The model performs well at both locations, with a slight tendency to underestimate the GTI UV relatively to the ground measurements. The results in Fig. 11 indicate RMSEs of 3.5–4.8 W/m^2 and MBEs of –2.5

TABLE III
COMPARISON OF RESULTS, USING DIFFERENT DEFINITIONS OF UV SPECTRAL RANGE

Station	NREL Model (280–400 nm)	NREL Model (295–400 nm)	Poliskie, 2011 (295–400 nm)	NREL Model (285–385 nm)	NREL Model (295–385 nm)	White et al., 2011 (295–385 nm)
Case Western Reserve Univ. (CWRU), Ohio, USA	291 (0° tilt)	288 (0°tilt)	—	227 (0°tilt)	224 (0°tilt)	—
	285 (5° tilt)	285 (5°tilt)		221 (5°tilt)	221 (5°tilt)	
	269 (41° tilt)	269 (41°tilt)		208 (41°tilt)	208 (41°tilt)	
Miami, Florida, USA	422 (0° tilt)	416 (0°tilt)		330 (0°tilt)	325 (0°tilt)	
	410 (5° tilt)	410 (5°tilt)		320 (5°tilt)	320 (5°tilt)	338 (5°tilt)
	400 (26° tilt)	400 (26°tilt)	390 (26°tilt)	304 (26°tilt)	311 (26°tilt)	
	369 (45° tilt)	369 (45°tilt)		295 (45°tilt)	288 (45°tilt)	320 (45°tilt)
NREL, Golden, Colorado, USA	341 (0° tilt)	339 (0°tilt)	—	266 (0°tilt)	264 (0°tilt)	—
	341 (5° tilt)	341 (5°tilt)		265 (5°tilt)	265 (5°tilt)	
	337 (40° tilt)	337 (40°tilt)		260 (40°tilt)	260 (40°tilt)	
Phoenix, Arizona, USA	439 (0° tilt)	436 (0°tilt)		343 (0°tilt)	340 (0°tilt)	
	435 (5° tilt)	435 (5°tilt)		339 (5°tilt)	339 (5°tilt)	359 (5°tilt)
	432 (34° tilt)	432 (34°tilt)	440 (34°tilt)	361 (34°tilt)	336 (34°tilt)	363 (34°tilt)

Notes: values (in MJ/m^2) are obtained using the NREL TMY dataset (NSRDB PSM V3); orientation is south facing in all cases.

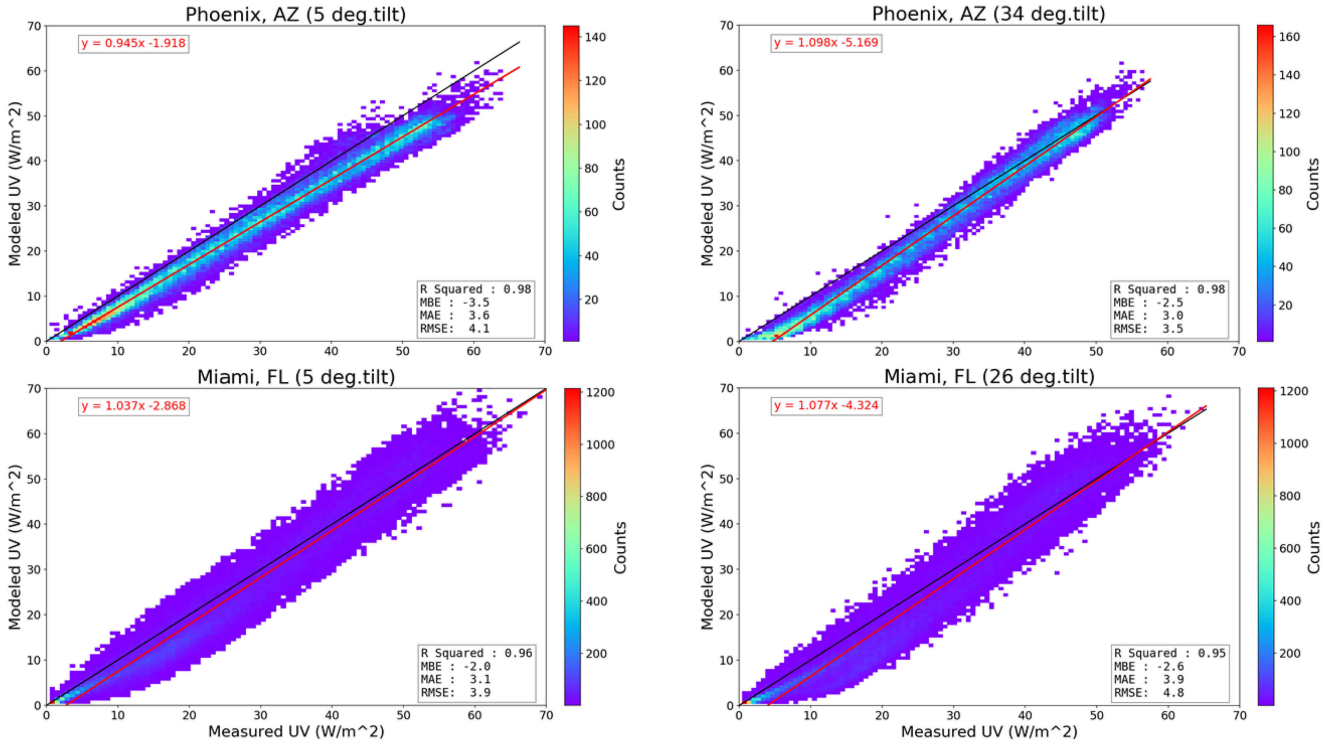

Fig. 11. Modeled versus measured GUV irradiance under all-sky conditions and various tilts. RMSE and MBE values are in W/m^2.

to 3.5 W/m^2 for the two locations and different tilts. There is more scatter at Miami than at Phoenix, possibly because of the prevalent tropical cloudiness of the former in summer. In the future, it will become possible to perform more validation at more locations, because of the expected availability of more sources of data for various tilts.

IV. CONCLUSION

A model was developed to estimate the GUV irradiance contained in multiple wavebands (280–400, 295–400, 285–385, and 295–385 nm) using the total broadband solar irradiance, TS, as obtained from usual radiation models or measured with, e.g., a conventional pyranometer. The method is based on simulations of both GUV and TS obtained with the SMARTS spectral radiation model. Under clear-sky conditions, the airmass factor was found to be the primary driver of the GUV/TS ratio, at least under "typical" atmospheric conditions. Further, still using SMARTS, the model was extended to estimate the GUV/TS ratio for a variety of tilt angles.

The proposed model can be applied to estimate the total UV irradiance from TS irradiance (GHI or GTI) under all-sky conditions. The necessary input data can be obtained from actual measurements, satellite-derived modeled time series, or usual TMY data files.

The preliminary tests reported here show that the modeled UV results are in good agreement with actual measurements at different time scales, multiple locations, and tilt angles, which

provides confidence about the accuracy of the model. The model typically under- or overestimates the measured UV irradiance within ± 2 W/m^2 only. The RMSE appears slightly better for the horizontal than the tilt results. This situation could be related to the model's limitation under tilted conditions, or to data quality of the input GTI data (which are estimated from GHI with a transposition model, thus adding uncertainty). As usual, the quality of the model's inputs largely conditions the UV predictions' accuracy.

The model proposed here is meant to characterize the UV irradiance or irradiation at any location, and hence to help understand the degradation of various materials used in PV modules, and ultimately to provide a reliable assessment of their service life. In this perspective, the model demonstrated results within 2–8% of the measured irradiance values on various tilts.

Additionally, the model does not seem to be significantly affected by cloudiness (except possibly at Miami), but appears sensitive to large excursions in AOD, PW or surface albedo, which will require further attention.

Further research will aim to improve the model by incorporating the effects of important variables, such as surface albedo, AOD or water vapor, so as to make it of more general validity.

Acknowledgment

The authors acknowledge the DOE Solar Energy Technologies Office and its Systems Integration subprogram for supporting this research. Specifically, they thank Dr. T. Golnas, Technology Manager of Systems Integration, for his support and encouragement. They are grateful to A. Andreas, I. Reda, M. Dooraghi, and M. Kutchenreiter for maintaining the world's largest array of web-accessible, continuously operating, radiometric measurements at the National Renewable Energy Laboratory's Solar Radiation Research Laboratory. They would also like to thank Dr. G. Bernhard from Biospherical Instruments, Inc., Dr. A. Kazantzidis from the University of Patras, Greece, M. McGreer from Atlas Material Testing Technology, and the reviewers for providing them data and insightful suggestions. This work was authored by Alliance for Sustainable Energy, LLC, the manager and operator of the National Renewable Energy Laboratory for the U.S. Department of Energy (DOE). The views expressed in the article do not necessarily represent the views of the DOE or the U.S. Government. The U.S. Government retains and the publisher, by accepting the article for publication, acknowledges that the U.S. Government retains a nonexclusive, paid-up, irrevocable, worldwide license to publish or reproduce the published form of this work, or allow others to do so, for U.S. Government purposes.

References

[1] *Standard Terminology Relating to Natural and Artificial Weathering Tests of Nonmetallic Materials*, ASTM G113-16, ASTM International, West Conshohocken, PA, USA, 2016, 5 pp.

[2] J. E. Pickett, M. Kenneth, M. White, and C. W. Christopher, "Chapter 1—Service life prediction: Why is this so hard?" in *Service Life Prediction of Polymers and Plastics Exposed to Outdoor Weathering*. Norwich, NY, USA: William Andrew Publishing (Plastics Design Library), 2018, pp. 1–18. [Online]. Available: https://doi.org/10.1016/B978-0-323-49776-3.00001-5

[3] CIE (International Commission on Illumination), "Rationalizing nomenclature for UV doses and effects on humans. Joint publication of CIE and WMO (World Meteorological Organization)," CIE (International Commission on Illumination), Vienna, Austria, Tech. Rep., CIE 209:2014—WMO/GAW Report no. 211, 2014.

[4] J. Wohlgemuth and S. Kurtz, "International PV QA Task Force's proposed comparative rating system for PV modules," *Proc. SPIE*, vol. 9179, pp. 917902-1–917902-8, 2014, doi: 10.1117/12.2067927.

[5] C. A. Gueymard, "Simple model of the atmospheric radiative transfer of sunshine, version 2 (SMARTS2): Algorithms description and performance assessment," Florida Sol. Energy Center, Cocoa, FL, USA, Tech. Rep. FSEC-PF-270-95, 1995.

[6] C. A. Gueymard, "Parameterized transmittance model for direct beam and circumsolar spectral irradiance," *Sol. Energy*, vol. 71, pp. 325–346, 2001.

[7] *Standard Tables for Reference Solar Spectral Irradiances—Direct Normal and Hemispherical on 37° Tilted Surface*, ASTM G173-03, ASTM International, West Conshohocken, PA, USA, 2012, 21 pp.

[8] C. J. Riordan, R. L. Hulstrom, and D. R. Myers, "Influences of atmospheric conditions and air mass on the ratio of ultraviolet to total solar radiation," Sol. Energy Res. Inst., Golden, CO, USA, Tech. Rep. SERI/TP-215-3895, 1990.

[9] G. Bernhard, C. R. Booth, and J. C. Ehramjian, "Version 2 data of the National Science Foundation's ultraviolet radiation monitoring network: South pole," *J. Geophys. Res.*, vol. 109, 2004, Art. no. D21207, doi: 10.1029/2004JD004937.

[10] W. Wandji *et al.*, "A new method for estimating UV fluxes at ground level in cloud-free conditions," *Atmos. Meas. Techn. Discuss.*, vol. 10, pp. 4965–4978, 2017, doi: 10.5194/amt-2017-223.

[11] A. Habte, M. Sengupta, A. Andreas, S. Wilcox, and T. Stoffel, "Intercomparison of 51 radiometers for determining global horizontal irradiance and direct normal irradiance measurements," *Sol. Energy*, vol. 133, pp. 372–393, 2016, doi: 10.1016/j.solener.2016.03.065.

[12] *Standard Tables for Reference Solar Ultraviolet Spectral Distributions: Hemispherical on 37° Tilted Surface*, ASTM G177-03, ASTM International, West Conshohocken, PA, USA, 2012, 10 pp.

[13] M. Poliskie, *Solar Module Packaging: Polymeric Requirements and Selection*. Boca Raton, FL, USA: CRC Press, 2011.

[14] C. C. White, *Service Life Prediction of Polymers and Plastics Exposed to Outdoor Weathering*. Saint Louis, MO, USA: William Andrew, 2017. [Online]. Available: http://lib.myilibrary.com?id=1039678

[15] *Standard Table for Reference Solar Spectral Distributions: Direct and Diffuse on 20° Tilted and Vertical Surfaces*, ASTM G197-14, ASTM International, West Conshohocken, PA, USA, 2014, 35 pp.

Authors' photographs and biographies not available at the time of publication.